Investigating Possible Causative Mechanisms for the Largest Hydraulic Fracturing Induced Earthquake in Canada

Bei wang[1,2], Alessandro Verdeccia[3], Honn Kao[1,2], Rebecca M. Harrington[4], and Hongyu Yu[1]

[1]Geological Survey of Canada, Natural Resources Canada

[2]School of Earth and Ocean Sciences, University of Victoria, Canada

[3]Department of Earth and Planetary Sciences, McGill University, Canada

[4]Institut für Geologie, Mineralogie und Geophysik, Ruhr-Universität Bochum, Germany

Summary

The Mw 4.6 earthquake that occurred on 17 August 2015 northwest of Fort St. John, British Columbia, is considered the largest hydraulic fracturing-induced event in Canada based on its spatiotemporal relationship with respect to nearby injection operations (Fig. 1). In this study, we have detected and estimated source parameters of more than 300 events proximal to the mainshock. Our results show that this Mw 4.6 earthquake occurred on a pre-existing fault with a stress drop value of ~35 MPa, typical of tectonic earthquakes. Meanwhile, we observe a ~5-day delay between this M_w 4.6 mainshock and the onset of fluid injection at the closest well pad (W1). In contrast, the other two injection sites in the vicinity (W2 and W3) have almost instantaneous seismic responses (Fig. 2). We take a forward numerical approach to investigate the causative mechanisms for this Mw 4.6 earthquake. Specifically, three finite-element 3D poroelastic models are constructed to calculate the coupled evolution of elastic stress and pore pressure caused by hydraulic fracturing fluid injections (Fig. 3). Our simulations suggest that the elastic stress perturbation caused by rock matrix deformation alone may not be sufficient to trigger the Mw 4.6 earthquake. Instead, a pore pressure increase associated with the migration of injected fluid could be the triggering mechanism of the mainshock. Furthermore, the stimulation work at W1 probably significantly altered the local stress field and brought local faults much closer to failure. This process can effectively shorten the seismic response time and thus explain the observed simultaneous appearance of injection and induced seismicity at W2 and W3.

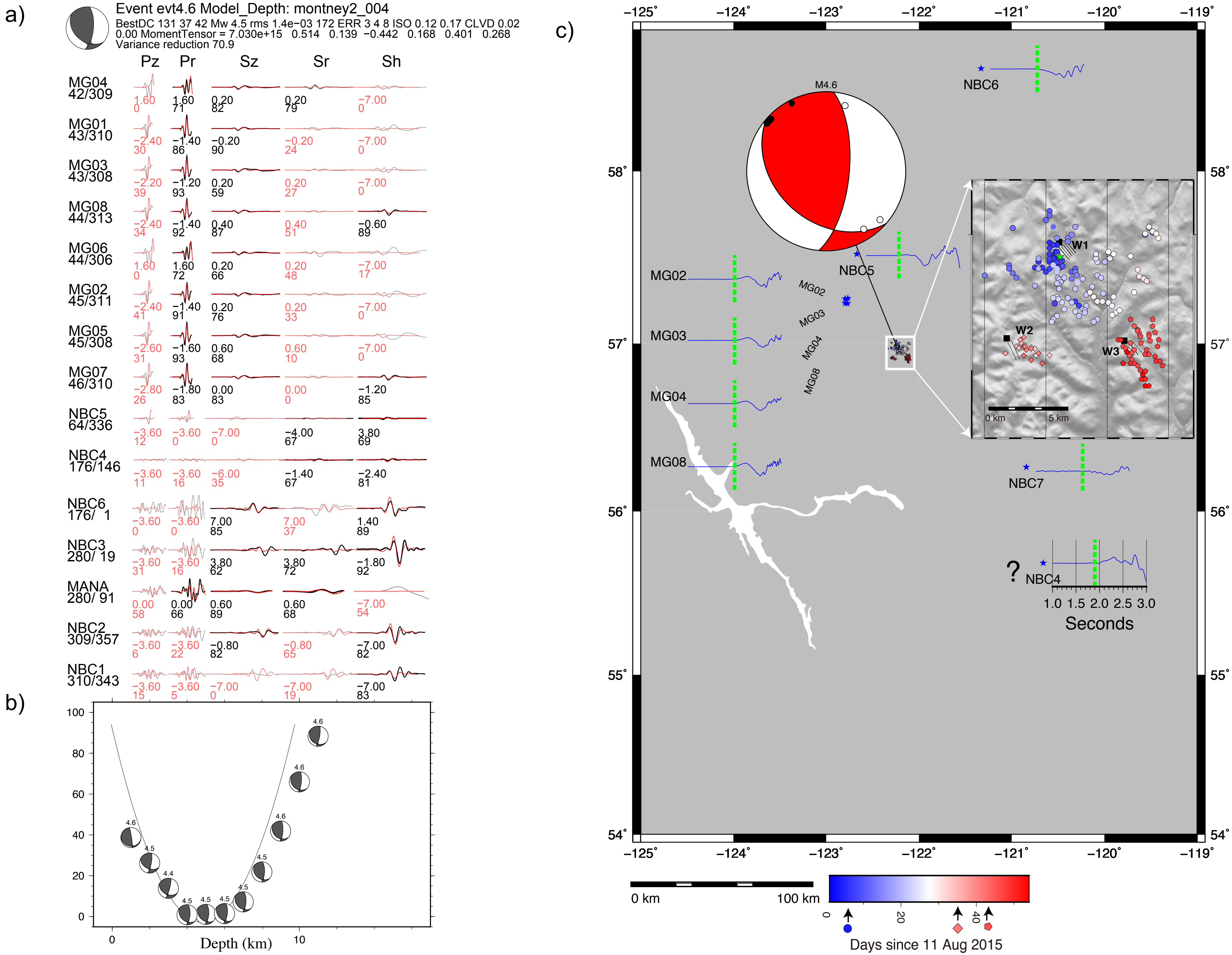

Figure 1. Focal mechanism solutions for the Mw 4.6 earthquake. a) synthetic and observed seismograms match at each station, which are plotted as dashed and solid lines, respectively. The lines with black numbers below show the used match in the inversion and lines with red numbers below are the discarded pairs. b) Misfit error of moment tensor inversion versus depth by gCAP method. c) The confidence check by the P-wave first motion method, where the black circles indicate stations with positive polarity (upward) and white circles indicate negative polarity (downward). The question mark at station NBC4 denotes that there is uncertainty for the polarity. The inset figure shows the seismicity during the HF period, symbol shapes differentiate clusters associated with respective HF wells, W1, W2, and W3.

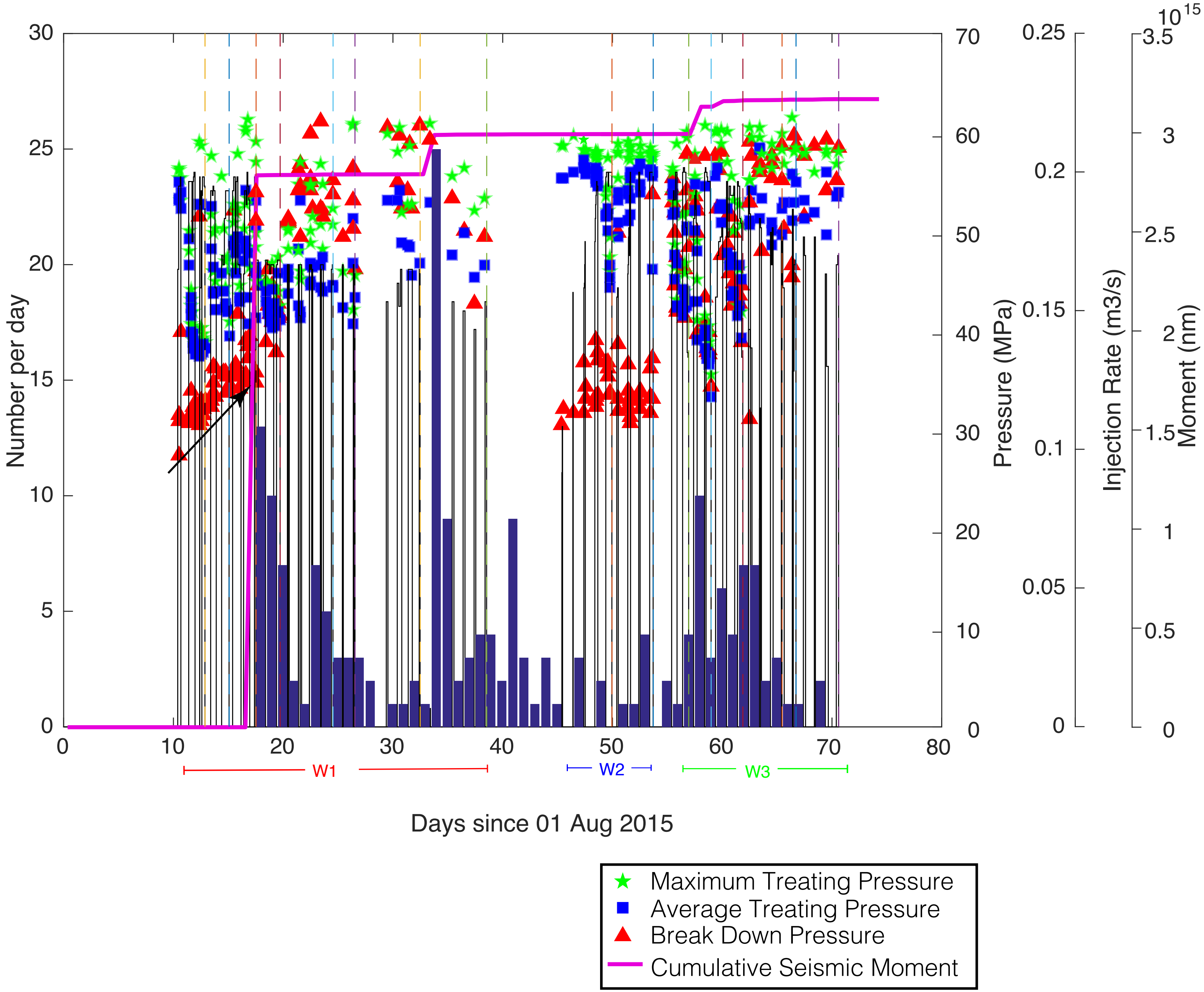

Figure 2. HF operation parameters, including maximum treating pressure, average treating pressure, breakdown pressure and injection rate. The blue bars denote the daily seismicity rate, and the purple line indicates the cumulative seismic moment. The thin lines represent the injection rate, and dashed lines denote the end time of each horizontal well.

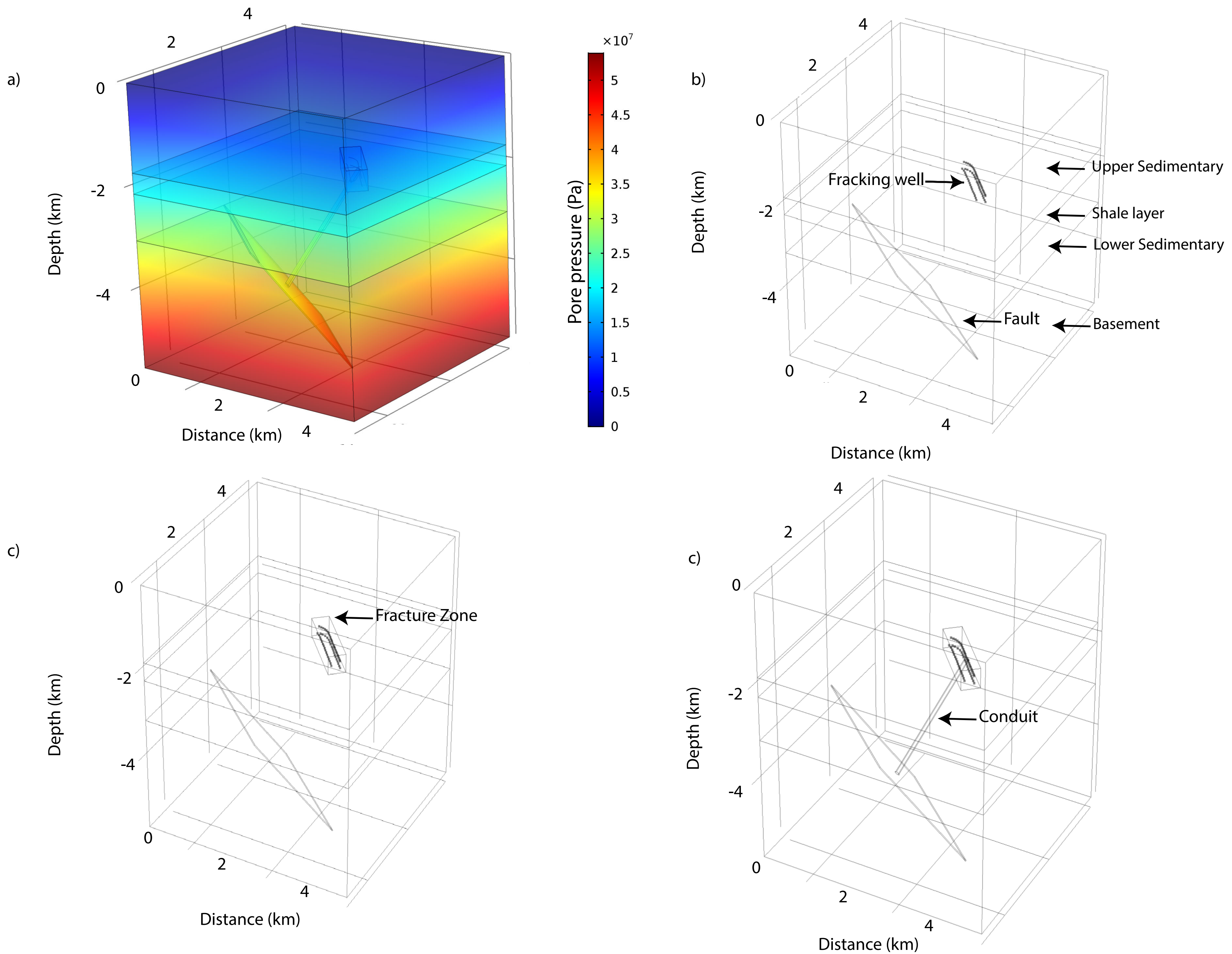

Fig.3 The four-layer model built with COMSOL to simulate the triggering mechanisms of the Mw 4.6 earthquake. a) The hydro-static pore pressure from the transient model before HF starts, which is used as the initial value input for the following time-dependent study. b) Model 1, the square in the fourth layer denotes the fault patch , the dashed points represent the injection points for each stage. c) Model 2, similar to Model 1, but with a high-permeable fracture zone caused by HF operation as indicated by the cube in the second shale layer. d) Model 3, similar to Model 2 but with a higher permeable conduit represented by the vertical cylinder. The properties for each layer and structure can be found in the Tab.S1.